

A New Wideband CPW-Vivaldi Antenna for the Detection of Breast Tumors in Microwave Imaging System

Fatemeh Geran^{1*}, Mohammad Bod¹ and Mohammad-Reza Darvish Khezri¹

Abstract— This paper presents a new wide-band CPW Vivaldi antenna for breast tumor detection. First, a simple CPW-fed Vivaldi antenna is designed based on two-term exponential equations. The coefficient of the exponential terms and the parameters of the antenna fed are optimized for the best impedance matching at the UWB frequency band. Then, peripheral slots are added to the antenna to improve the impedance matching and gain. A prototype of this antenna is fabricated, and the scattering parameters and radiation patterns are measured. The proposed antenna achieves a wide bandwidth of 2.9–10.8 GHz with a VSWR < 3.5 and 4.2–10.2 GHz with a VSWR < 2, along with a peak gain exceeding 1 dBi. Finally, microwave imaging with the help of six samples of the proposed antenna is done. An image of a cancerous tissue inside a breast is reconstructed using the delay and sum method, successfully detecting a 20 mm spherical tumor. All the results show that a suitable antenna for a microwave imaging system is proposed.

Keywords—Vivaldi antenna, CPW antenna, microwave imaging, wideband, breast cancer

I. INTRODUCTION

In recent years, numerous studies have been reported on the early detection of various types of cancer using different frequency ranges, including microwave, terahertz, and optical frequencies. For example, terahertz imaging has shown promise in detecting skin cancer due to its high sensitivity to water content and cellular changes [1]. Similarly, optical coherence tomography (OCT) has been widely used for early-stage cancer diagnosis, offering high-resolution imaging of superficial tissues [2]. Microwave imaging, on the other hand, is particularly advantageous for detecting deeper tumors, such as those in breast tissue, due to its ability to penetrate dense tissues and provide information about dielectric properties [3]. This diversity in imaging techniques highlights the importance of selecting the appropriate frequency range and methodology based on the specific application and target tissue.

Microwave imaging involves sending microwave signals toward a target and analyzing the reflected or scattered signals to generate an image of the object or structure. This method relies on different materials' varying microwave interaction properties to distinguish between different objects or tissues [1]. Microwave imaging applications span multiple fields, including medical imaging, non-destructive testing, security screening, geological exploration, and environmental monitoring. Fig. 1 provides further details regarding the diverse applications of microwave imaging.

This study focuses on the medical application of microwave imaging technology. The potential of microwave imaging in the early detection of breast cancer tumors offers

hope for more effective methods of combating breast cancer mortality and achieving complete treatment in a shorter period [1]. The first research on microwave imaging hardware systems in biomedicine dates back to the late 1970s. In the design presented by Jacobi and Larsen, they measured the amplitude and phase of the transmission coefficient of a 3.9 GHz band microwave signal between two moving horn antennas (one as a transmitter and the other as a receiver) located on both sides of the dog's isolated kidney. Finally, they obtained an image of the dog's kidney by analyzing the data [5]–[6].

In the early 1990s, a circular microwave imaging system was developed. This structure, with antennas placed circularly around the target tissue, produces superior results in image reconstruction compared to linear antenna placement [7]. The promising results from this research have inspired various groups to develop further and expand other systems [8]–[9].

Microwave devices such as filters [10]–[12], sensors [13], [14], and antennas [15]–[23] play a role in the microwave imaging systems. Among them, antennas are the most important element in microwave imaging systems for tumor detection. The antenna must have a directional radiation pattern with high gain to reduce backward radiation and noise. The antenna must have a directional radiation pattern with high gain to reduce backward radiation and noise. The antenna should also be easily integrated with imaging systems and placed around the body tissue. Therefore, it should be as compact as possible. Based on these specifications, the Vivaldi antenna is a good candidate for microwave imaging systems and has been widely used in recent works [15]–[22].

Vivaldi antennas not only have a directional pattern but also a fixed phase center over a broad frequency band. This characteristic helps microwave imaging systems work on a broad frequency band and create a high-resolution image. Most recent work on microwave imaging systems with Vivaldi antennas is done in ultra-wideband frequencies (UWB) of 3.1 to 10.6 GHz.

Due to these challenges, the attention and focus of many researchers have increased to improve this characteristic of Vivaldi antennas. Various methods have been used to improve the Vivaldi antenna characteristics as follows:

- The use of metamaterial structures [15], [16].
- Using a cavity as the back structure of the antenna [17].
- The use of rectangular slots alternately on the arms of the metal part [18].
-
- By special shaping of the substrate, a lens-like shape is created at the end of the antenna, which is used to increase Vivaldi antennas' directionality [19].

1. Faculty of Electrical Engineering of Shahid Rajaei Teacher Training University, Tehran, Iran.

* Corresponding author: Email: f.geran@sru.ac.ir

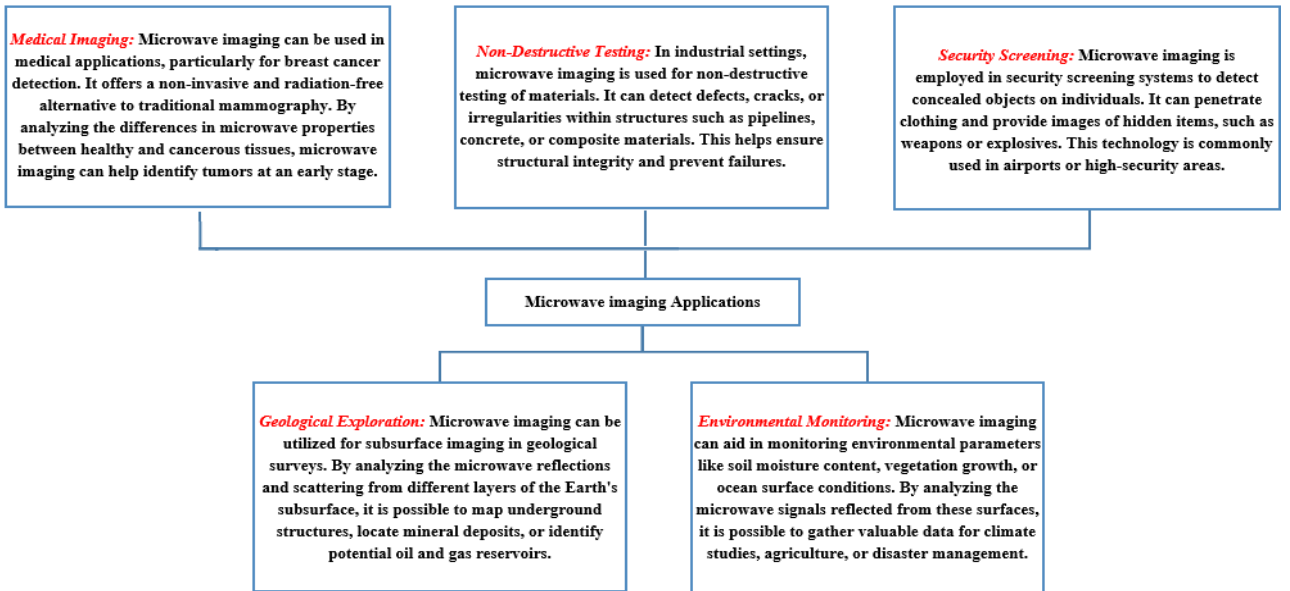


Fig. 1: The types of microwave imaging applications.

- The use of array structures of Vivaldi antennas [20].
- The use of unique designs for the part of the metal arms of the antenna or structures with different designs in the antenna feeding part [21],[22].
- Using directional structures. These structures are made of cut shapes from materials with high dielectric coefficients and are placed in the end part of the antenna [23].

This paper presents an improved CPW-fed Vivaldi antenna for a microwave imaging system. First, a simple CPW-fed Vivaldi antenna is designed based on two-term exponential equations. The coefficient of the exponential terms and the parameters of the antenna feed are optimized for the best impedance matching at the UWB band. Another example of the CPW antenna with peripheral slots is also designed to improve the impedance matching and the antenna gain. A prototype of the second design is fabricated, and the measured results are compared with the full-wave results of HFSS software. Finally, microwave imaging with the help of six samples of the Vivaldi antenna is done in the Msoftware. After collecting the coupling matrix, the image of a cancerous tissue inside the breast is reconstructed using the delay and sum method. All the results show that a suitable antenna for a microwave imaging system has been created. The paper is organized in four sections. In the second section, the proposed antenna and its results are presented. In the third section, the simulation and measurement results of the proposed antenna and the method of tumor detection are introduced, and finally, in the fourth section, the summary of the article is presented.

II. ANTENNA DESIGN

Coplanar Waveguide (CPW) lines offer several advantages over other transmission lines, making them popular in many high-frequency applications. CPW lines are easy to fabricate on planar substrates, allowing integration with other circuit elements. They have low radiation losses, which is crucial for minimizing signal degradation. Additionally, CPW lines provide good impedance control, enabling precise matching to other components. Their symmetrical structure helps to reduce crosstalk between adjacent lines, ensuring clean signal transmission.

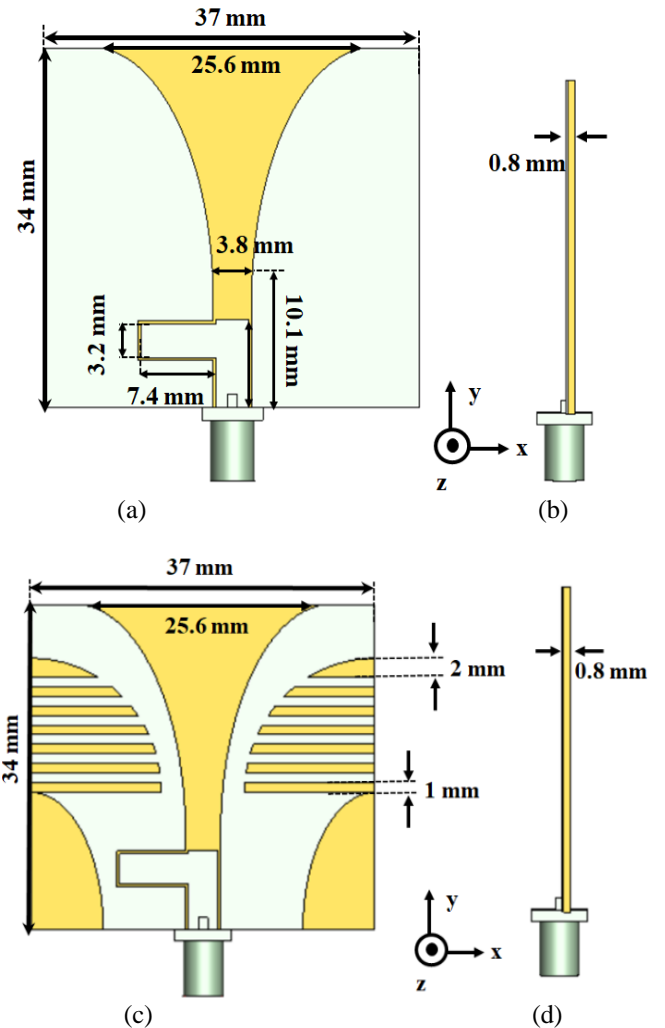


Fig. 2 The proposed CPW-fed Vivaldi antenna based on two-term exponential equations (a) Top view of simple CPW-fed Vivaldi antenna (Design I), (b) side view of Design I, (c) Top view of CPW-fed Vivaldi antenna with peripheral slots, (Design II), (d) Side view of Design II.

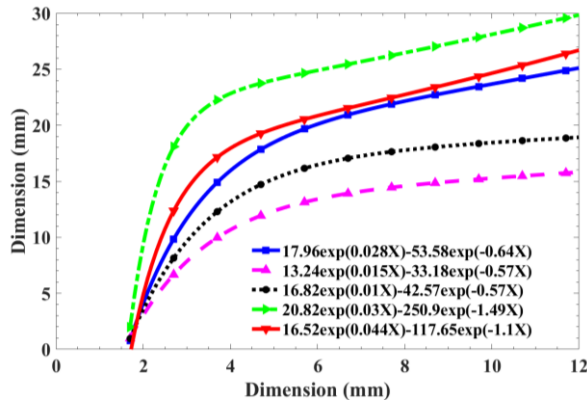


Fig. 3. Different shapes of Vivaldi antenna opening based on choosing different values for A, B, C, and D coefficients.

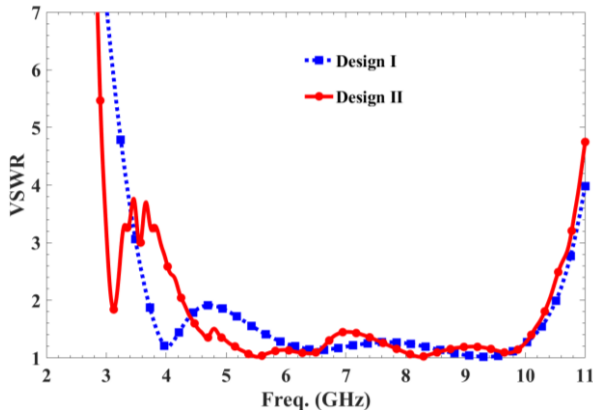


Fig. 4. The simulated VSWR of the simple CPW-fed Vivaldi antenna based on two-term exponential equations (Design I) and the CPW-fed Vivaldi antenna with peripheral slots (Design II)

A CPW-fed Vivaldi antenna is a type of broadband Vivaldi antenna that utilizes a CPW line as its feeding element. The antenna's geometry resembles a tapered wedge, with the CPW line widening towards the end. This gradual taper allows the antenna to operate over a wide range of frequencies. A CPW-fed Vivaldi antenna has several advantages over the traditional antenna. It has a more straightforward design, which makes it easier to fabricate and integrate into systems. It also has better impedance matching and lower insertion loss, which improves its performance. Also, CPW Vivaldi antennas are known for wide bandwidth, high gain, and ease of fabrication, making them an ideal choice for microwave imaging applications.

Based on this fact, a CPW-fed Vivaldi antenna is designed in Fig.2. As seen in this figure, the proposed Vivaldi antenna consists of an L-shaped CPW feed line and a tapered opening slot. The proposed antenna is placed on an FR4 board with a dielectric constant of 4.4 and a dielectric loss tangent of 0.02. The overall dimensions of the antenna are $34 \times 37 \text{ mm}^2$ with a thickness of 0.8 mm. There is a 50-ohm SMA connector at the antenna input. Also, the input CPW line has a width of 3.2 mm and a gap of 0.3 mm, which is adapted to the 50-ohm impedance of the connector.

The radiating part of the Vivaldi antenna consists of a fixed section with a width of 3.8 mm and a length of 10.1 mm. After that, the opening slot is based on a two-term exponential equation.

The two-term exponential equation is defined as follows:

$$Y = Ae^{BX} + Ce^{DX} \quad (1)$$

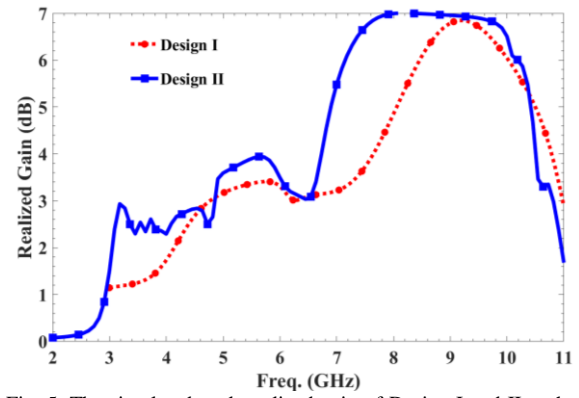


Fig. 5. The simulated peak realized gain of Design I and II at the end fire angle ($\theta=90^\circ$, $\phi=90^\circ$ degree according to the cartesian coordinates shown in Fig. 2).

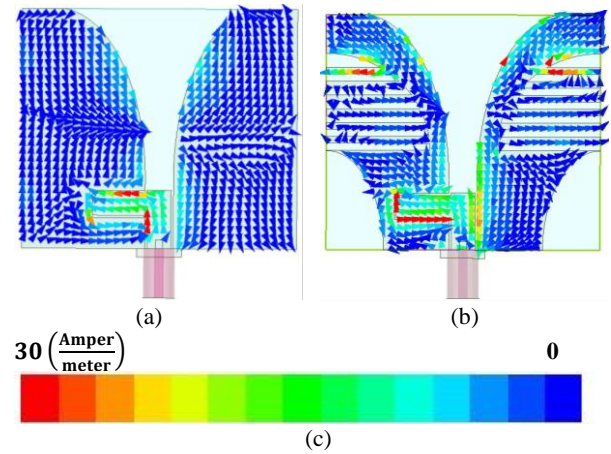


Fig. 6. The simulated surface current of a) Design I, b) Design II at 6.5 GHz frequency, and c) the current scale for both antennas.

In which X and Y are the coordinates according to Fig. 2, and A, B, C, and D are the coefficients of the exponential term. Different tapering shape coefficients can be obtained based on their different values.

Fig. 3 shows the different tapering shapes obtained with A, B, C, and D coefficients in equation (1). In fact, with different selections of the exponential equation coefficients, the Vivaldi antenna's opening changes. This opening directly affects the impedance matching of the proposed antenna. In an optimization algorithm in the HFSS software, A, B, C, and D coefficients in equation (1), along with L-shaped line parameters, were optimized to have the best impedance matching in the UWB band. Based on this optimization, the length of the L-shaped CPW line is obtained as 7.4 mm, and the parameters of the tapered section are obtained as follows: $A = 17.96$, $B = 0.028$, $C = -53.58$, $D = -0.64$.

To improve the performance of the proposed antenna and increase the gain, another CPW Vivaldi antenna with a two-term exponential equation is presented in Fig. 2 (c) and (d). We named this scheme as design II in this paper. As shown in Fig. 2, seven peripheral slots have been inserted on both sides of the Vivaldi radiation section. Each of these slots has a width of about 1 mm, except the two-ended slots, which have a 2 mm width. The dimensions of this antenna are selected similarly to the previous one, as $34 \times 37 \times 0.8 \text{ mm}^3$.

The L-shaped CPW fed, and the Vivaldi curve remain unchanged. In the next section, it will be shown that the

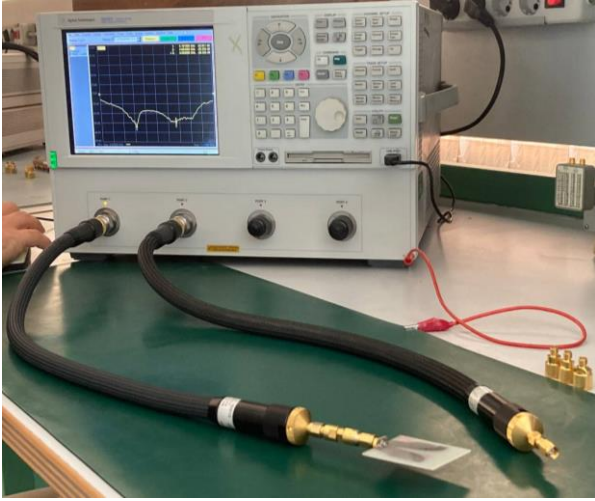


Fig. 7. The measurement of Design II antenna with Agilent network N5230A.

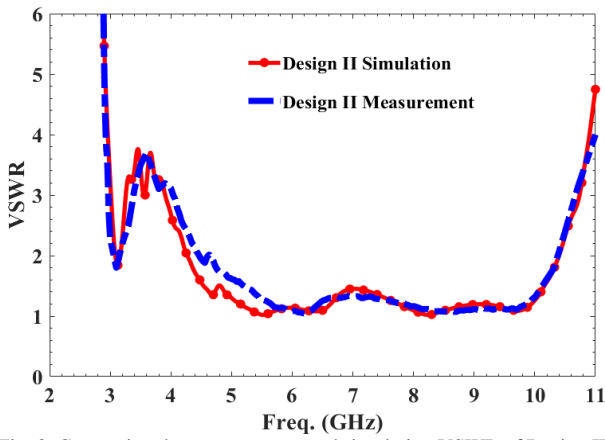


Fig. 8. Comparing the measurement and simulation VSWR of Design II antenna.

peripheral slots strengthen the radiation current of the antennas and increase the antenna gain in the UWB band.

III. RESULTS AND DISCUSSION

A. Antenna Results

In this section, the simulation and measurement results of the proposed antenna are studied. First of all, the simulated VSWR of the simple CPW-fed Vivaldi antenna based on two-term exponential equations (Design I) and the CPW-fed Vivaldi antenna with peripheral slots (Design II) are shown in Fig. 4. As can be seen, Design I covers 3.5 to 10.9 GHz frequency. In contrast, Design II covers 2.9 to 10.8 GHz, with $VSWR < 3.5$. Many transmitters work well with VSWR around 3; however, both antennas in the 4.2-10.2 GHz frequency range have VSWRs better than 2 and are very close to 1.

The simulated realized gain of both Design I and II are shown in Fig. 5. In this figure, the realized gains are evaluated at the end fire angle, i.e. $\theta=90^\circ$, $\phi=90^\circ$ degree according to the cartesian coordinates shown in Fig. 2. As can be seen, the realized gain of both antennas are varying from 1 – 7 dB at 3-11 GHz in both antennas. However, the peak realized gain of Design II is significantly better than that of Design I. This increase in gain is because the peripheral slots have caused better impedance matching of the antenna of the second design at some frequencies. Therefore, the realized gain of the antenna has improved.

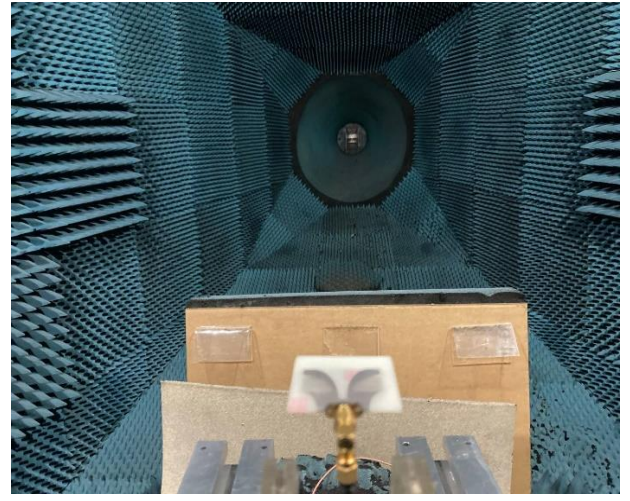


Fig. 9. Measuring the radiation pattern of Design II antenna in the Anechoic chamber.

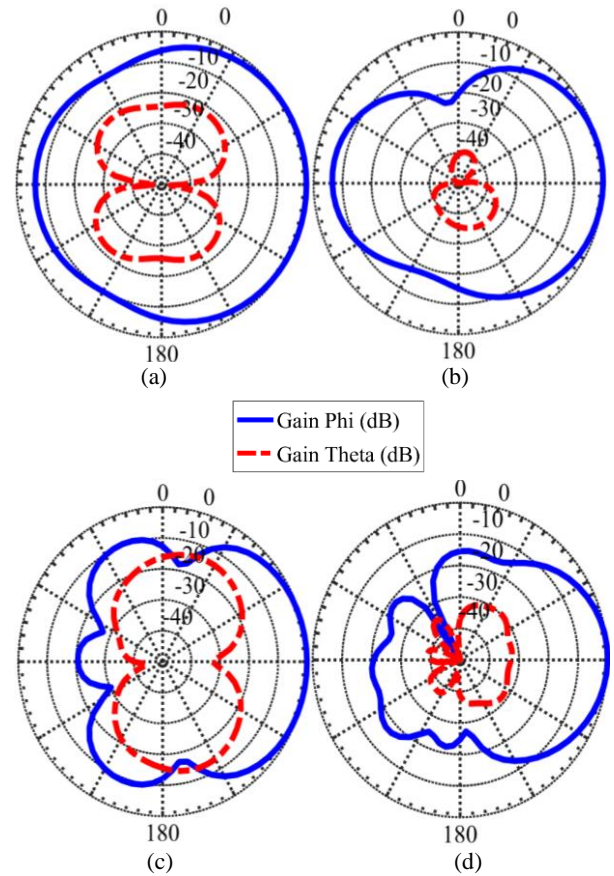


Fig. 10. Normalized radiation pattern of the proposed antenna (Design II) at a) $\phi=90^\circ$ 4GHz frequency, b) $\theta=90^\circ$ 4GHz frequency, c) $\phi=90^\circ$ 8GHz frequency, b) $\theta=90^\circ$ 8GHz frequency.

To better evaluate the performance of the two presented designs, in Fig. 6, the surface current of designs I and II at the frequency of 6.5 GHz is shown. As can be seen in Design I, the surface currents are concentrated around the CPW feed and tapered Vivaldi curve. Design II also has a high-intensity surface current around the peripheral slots. These slots increase the electrical length of the antenna of Design II; therefore, the working frequency of the second antenna decreases. This issue was also investigated in Fig. 4. As mentioned before, the working frequency of Design II has decreased from 3.5 GHz to 2.9 GHz.

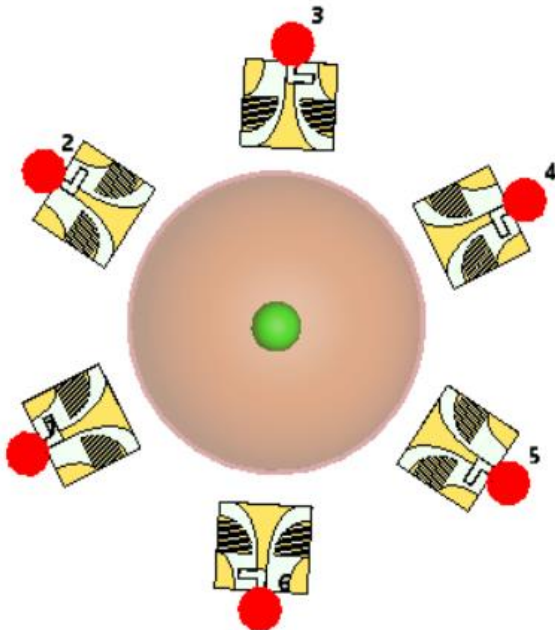


Fig. 11. Placement of six of the proposed antennas around the breast tissue with the cancerous tumor in its center.

A prototype of the Design II antenna is fabricated, and its VSWR is measured with Agilent network N5230A at Iran Telecommunication Research Center (ITRC), as shown in Fig. 7. As can be seen, the results of simulation and measurement perfectly match the desired band.

The radiation pattern of the fabricated antenna is also measured in E- and H-planes. Fig 9 shows how to perform the test in the anechoic chamber of the Iran Telecommunication Research Center. The normalized radiation patterns of the proposed antenna are shown in Fig. 10. This figure plots radiation patterns at two frequencies of 4 and 8 GHz at the $\phi = 90^\circ$ (H-plane) and $\theta = 90^\circ$ (E-plane). As can be seen, the antenna has a directional pattern in both planes. Also, the differences between the co-polarization and the cross-polarization in both frequencies and planes are more than 30 dB.

B. Microwave Imaging results

This section will examine microwave imaging with the proposed antenna. For this purpose, a breast phantom, which includes two layers of skin and fat, is considered first. The thickness of the skin layer is 2 mm with a dielectric constant of 36 and conductivity of 4 S/m. The fat layer has a diameter of 116 mm with a dielectric constant of 9 and a conductivity of 0.4 S/m. In the middle of this phantom, there is a spherical tumor tissue with a diameter of 20 mm. This tumor has a dielectric constant of 50 and a conductivity of 4 S/m. According to Fig. 11, around the under-test phantom, six antennas are placed with an angular distance of 60 degrees.

To reconstruct the image in this problem, the open-source code MERIT is used. MERIT is a MATLAB code based on the delay and sum method [24]-[26]. In this method, each of the six antennas acts as the transmitter and the reception is stored in the other five antennas with scattering parameters. Due to the reciprocity between transmitter and receiver antennas, only 16 mutual-scattering matrices are needed for reconstructing the image. Each scattering matrix element

contains 1000 frequency samples in the UWB band. The scattering matrix is calculated in two steps to remove reflection from the skin. In the first step, the location of the antennas is the same as in Fig. 11, and in the second step, all the antennas are rotated 30 degrees from the center of the tissue.

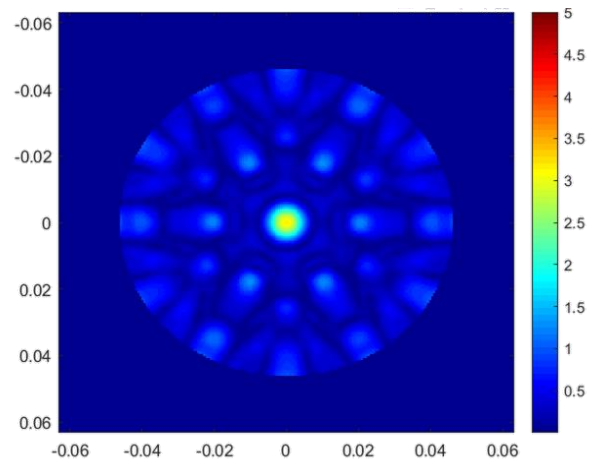


Fig. 12. The reconstructed image of breast cancer and identifying of the tumor at the center of the breast.

After collecting the scattering matrices between the antenna elements and determining the antennas' location, the data is entered into the MERIT code. The result obtained from the cancerous tissue and breast phantom is shown in Fig. 12. As can be seen, the cancerous tissue in the middle of the tissue is well separated from the background fat. If this process is repeated with more antennas, images with better clarity and less ambiguity can be achieved. Finally, based on the results obtained in this paper, it is clear that the proposed antenna is a suitable candidate for microwave imaging in the UWB frequency band.

C. Comparison with other works

The proposed CPW-fed Vivaldi antenna demonstrates competitive performance compared to other state-of-the-art designs, as summarized in Table I. While some designs achieve higher gain or larger bandwidth, the proposed antenna stands out for its compact size ($34 \times 37 \text{ mm}^2$) and optimized impedance matching across the UWB band. These features make it particularly suitable for integration into microwave imaging systems for breast tumor detection. Additionally, the use of peripheral slots improves gain and impedance matching, addressing a common challenge in Vivaldi antenna design. Future work will focus on further miniaturization and gain enhancement to improve its performance for clinical applications.

While the proposed CPW-fed Vivaldi antenna demonstrates promising performance for breast tumor detection, several limitations and challenges must be acknowledged. The antenna's performance is optimized for the UWB frequency range (2.9–10.8 GHz), which may not be suitable for all breast tissue types, particularly dense tissues requiring lower frequencies for deeper penetration.

TABALE I
Comparison of the Proposed Design With Other Similar Works

Reference	Antenna Type	Frequency Range (GHz)	Bandwidth (GHz)	Peak Gain (dBi)	Size (mm ²)	Application
Proposed Design	CPW-fed Vivaldi	2.9–10.8	7.9	7	34 × 37	Breast tumor detection
Zhou & Cui [15]	Metamaterial-loaded Vivaldi	3–14	11	9.5	140 × 80	UWB applications
Bai et al. [17]	Cavity back Vivaldi	2.5–8.5	6	8.5	63 × 51	Microwave breast imaging
Teni et al. [18]	Miniaturized antipodal Vivaldi	4–30	26	6	66 × 50	UWB applications
Bourqui et al. [23]	Balanced antipodal Vivaldi	2.4–18	15.6	N/A	80 × 44	Near-field microwave imaging
Samsuzzaman et al. [26]	Modified antipodal Vivaldi	2.5–11	10	7.2	40 × 40	Microwave breast imaging

Additionally, the near-field operation introduces challenges such as coupling effects and sensitivity to antenna placement. The current system uses six antennas, limiting imaging resolution for smaller tumors (<10 mm). Future work should focus on multi-frequency operation, advanced image reconstruction algorithms, and in vivo testing to address these limitations and improve clinical applicability.

IV. CONCLUSION

Cancer and breast tumor diagnosis have been investigated by microwave imaging methods using novel CPW-fed Vivaldi antennas. At the beginning of the paper, an ultra-broadband Vivaldi antenna with suitable performance characteristics has been designed to use the microwave imaging method. To improve the impedance matching of the proposed Vivaldi antenna, peripheral slots are added to the antenna. This antenna was fabricated, and the measurement results matched the simulation well. The proposed antenna can cover 2.9–10GHz with a VSWR less than 3.5 and 4.2–10.2 GHz with a VSWR less than 2. The peak gain of the proposed antenna in the UWB band is more than 1dBi. An imaging result with the six examples of the proposed antenna was also obtained. The imaging was done with the MERIT open-source code based on the delay and sum algorithm. The results show that the code can perfectly identify tumor tissue in the background of a fat breast. Based on these results, it is clear that the proposed antenna is a suitable candidate for microwave imaging in the UWB frequency band.

REFERENCES

- [1] P. Zamzam, P. Rezaei, S.A. Khatami, and B. Appasani, "Super perfect polarization-insensitive graphene disk terahertz absorber for breast cancer detection using deep learning," *Optics & Laser Technology*, 183, p.112246, 2025.
- [2] Liu, X., Cui, M., Feng, C., Jin, S., Han, X., Wu, Y., Meng, D., Zuo, S., Xu, Q., Tai, Y. and Liang, F., "Clinical evaluation of breast cancer tissue with optical coherence tomography: key findings from a large-scale study," *Journal of Cancer Research and Clinical Oncology*, vol. 151, no. 2, pp.1-13, 2025.
- [3] S. Vaezi, P. Rezaei, A. A. Khazaei, "A Dual IoT/ISM Smart Glasses Antenna with Human Health Concern," *Iran J Sci Technol Trans Electr Eng*. Vol. 48, pp. 1553–1566, 2024.
- [4] M. O'Halloran, M. Glavin, and E. Jones, "Rotating antenna microwave imaging system for breast cancer detection," *Progress in Electromagnetics Research*, vol. 107, pp. 20.2010
- [5] J. Bolomey, A. Izadnegahdar, L. Jofre, Ch. Pichot, G. Peronnet, and M. Solaimani, "Microwave diffraction tomography for biomedical applications," *IEEE Transactions on Microwave Theory and Techniques*, Vol. 30, no.11, pp.1998–2000, Nov 1982.
- [6] G. Peronnet, Ch Pichot, J. Bolomey, L. Jofre, A. Izadnegahdar, C. Szeles, Y. Michel, J.L. Guerquin-Kern, and M. Gautherie, "A microwave diffraction tomography system for biomedical applications," *Microwave Conference*, 1983. 13th European, pages 529–533, Sept 1983.
- [7] A. Franchois and C. Pichot, "Microwave imaging-complex permittivity reconstruction with a Levenberg-Marquardt method," *IEEE Transactions on Antennas and Propagation*, I, 45(2):203–215, Feb 1997.
- [8] S.Y. Semenov, R.H. Svenson, A.E. Boulyshev, A.E. Souvorov, V.Y. Borisov, Y. Sizov, A.N. Starostin, K.R. Dezern, G.P. Tatsis, and V.Y. Baranov, "Microwave tomography: two-dimensional system for biological imaging," *Biomedical Engineering, IEEE Transactions on*, 43(9):869–877, Sept 1996.
- [9] P.M. Meaney, K.D. Paulsen, A. Hartov, and R.K. Crane, "An active microwave imaging system for reconstruction of 2-d

- electrical property distributions," Biomedical Engineering, IEEE Transactions on, 42(10):1017–1026, Oct. 1995.
- [10] S. Khani, S.M.H., Mousavi, M. Danaie, and P. Rezaei, "Tunable compact microstrip dual - band bandpass filter with tapered resonators," Microwave and Optical Technology Letters, 60(5), pp.1256-1261, 2018.
 - [11] M. Bod, and S. M. Hashemi, "Design of a Compact UWB Filter with Low Insertion Loss and High Selectivity," IETE Journal of Research, vol. 70, no. 5, pp. 4415–4421, 2023.
 - [12] S. Khani, S. V. A. D. Makki, S. M. H. Mousavi, M. Danaie, and P. Rezaei, "Adjustable compact dual - band microstrip bandpass filter using T - shaped resonators," Microwave and Optical Technology Letters, vol. 59, no. 12, pp.2970-2975, 2017.
 - [13] A. Ebrahimi, J. Scott and K. Ghorbani, "Differential Sensors Using Microstrip Lines Loaded with Two Split-Ring Resonators," IEEE Sensors Journal, vol. 18, no. 14, pp. 5786-5793, 15 July 2018.
 - [14] J. W. Sanders, J. Yao and H. Huang, "Microstrip Patch Antenna Temperature Sensor," IEEE Sensors Journal, vol. 15, no. 9, pp. 5312-5319, Sept. 2015.
 - [15] B. Zhou and T. J. Cui, "Directivity enhancement to Vivaldi antennas using compactly anisotropic zero-index metamaterials," IEEE Antennas and Wireless Propagation Letters, vol. 10, pp. 326-329, 2011.
 - [16] M. Bhaskar, Z. Akhter, S. L. Gupta, and M. J. Akhtar, "Design of anisotropic zero-index metamaterial loaded tapered slot Vivaldi antenna for microwave imaging," IEEE in Antennas and Propagation Society International Symposium (APSURSI), pp. 1594-1595, 2014.
 - [17] M. Abbak, M. Çayören, I. Akduman, "Microwave breast phantom measurements with a cavity-backed vivaldi antenna," IET Microw. Antenna. P. vol. 8, no.13, pp. 1127-1133, 2014.
 - [18] G. Teni, N. Zhang, J. Qiu, and P. Zhang, "Research on a novel miniaturized antipodal Vivaldi antenna with improved radiation," IEEE Antennas and Wireless Propagation Letters, vol. 12, pp. 417-420, 2013.
 - [19] K. Kota and L. Shafai, "Gain and radiation pattern enhancement of balanced antipodal Vivaldi antenna," Electronics Letters, vol. 47, pp. 303-304, 2011.
 - [20] E. W. Reid, L. Ortiz-Balbuena, A. Ghadiri, and K. Moez, "A 324-element Vivaldi antenna array for radio astronomy instrumentation," Instrumentation and Measurement, IEEE Transactions on, vol. 61, pp. 241-250, 2012.
 - [21] Y. Wang, G. Wang, X. Gao, and C. Zhou, "Double-slot Vivaldi antenna with improved gain," Electronics Letters, vol. 49, pp. 1119-1121, 2013.
 - [22] J. Wu, Z. Zhao, Z. Nie and Q. -H. Liu, "A Printed UWB Vivaldi Antenna Using Stepped Connection Structure Between Slotline and Tapered Patches," in IEEE Antennas and Wireless Propagation Letters, vol. 13, pp. 698-701, 2014.
 - [23] J. Bourqui, M. Okoniewski, and E. C. Fear, "Balanced antipodal Vivaldi antenna with dielectric director for near-field microwave imaging," IEEE Transactions on Antennas and Propagation, vol. 58, pp. 2318-2326, 2010.
 - [24] D. O'Loughlin et al., "Open-source software for microwave radar-based image reconstruction," 12th European Conference on Antennas and Propagation (EuCAP 2018), London, UK, pp. 1-4, 2018.
 - [25] D. O'Loughlin, B. L. Bárbara Oliveira, M. Glavin, E. Jones and M. O'Halloran, "Effects of Interpatient Variance on Microwave Breast Images: Experimental Evaluation," 40th Annual International Conference of the IEEE Engineering in Medicine and Biology Society (EMBC), Honolulu, HI, USA, 2018, pp. 5660-5663, 2018.
 - [26] M. Samsuzzaman, M. T. Islam, A. A. Shovon, R.I. Faruque, and N. Misran, "A 16-modified antipodal Vivaldi antenna array for microwave-based breast tumor imaging applications," Microwave and Optical Technology Letters, vol. 61, no. 9, pp.2110-2118, 2019.